

Numerical Study of the Wake Flow of a Wind Turbine with Consideration of the Inflow Turbulence

Xiaoyu Luo ^a, Qiuming Li ^b, Shishu Xiong ^b, Zhenqing Liu ^{b*}

^a Electric Power Research Institute of Guangdong Power Grid Co., Ltd., Guangzhou, Guangdong, China.

^b School of Civil Engineering and Mechanic, Huazhong University of Science and Technology, Wuhan, China.

Received 31 May 2018; Accepted 30 July 2018

Abstract

Considering the fact that wind turbines operate at the bottom of the atmospheric boundary layer (ABL) where the turbulence is at a high level, and the difficulty of mesh generation in the fully modeled numerical simulation, it is necessary to carry out researches to study the wake flow of wind turbines with consideration of the inflow turbulence. Therefore, a numerical method generating turbulence was proposed and the results show good agreement with those in experiments, based on which the flow fields in the wake of a wind turbine at two tip speed ratios are examined in detail through three actuator methods, namely, ADM, ADM-R and ALM. The performances of these methods were studied and the error sources for each method are clarified. Moreover, the computational efficiency were revealed and the influencing factor for the efficiency is concluded. Besides, the equilibrium relation of the N-S equation in the wake is revealed, which provides a theoretical basis for the optimal arrangement of the wind turbine. It shows that the mean velocity and fluctuating velocity vary greatly near the wind turbine, and become stable gradually away from the wind turbine. The results of ALM method shows the best agreement with the experiment. At near wake region, the turbulent stress term, pressure gradient term and convection term mainly contribute to the equation equilibrium, and convection term is in equilibrium with the turbulent stress term at the far wake.

Keywords: Actuator Disk; Actuating Line; Wind Turbines Wake; CFD; Numerical Simulation.

1. Introduction

With the increasing demand for clean, safe and cheap energy, wind power has been expanding globally in recent years and it has become a dominant renewable energy source, with over 280 GW installed worldwide by the end of 2012. In general, wind turbines are installed in wind farms along several rows and columns. Because wind turbines generate wakes that propagate downwind, the wakes from turbines in upwind rows can negatively impact the performance of downwind rows. Understanding wake losses is therefore an increasingly important topic as wind farms grow in size and in number of turbine rows. The energy loss caused by wake has a great effect on the economic benefit of wind farm. Therefore, the study of wind turbine wakes plays an important role in improving the efficiency of wind turbine power generation.

The wind tunnel test and CFD numerical simulation are the main research methods of wind turbine wakes. It's controllable and predictable for the experimental environment, which is the unique advantages of wind tunnel test. The disadvantage of wind tunnel test is that there is a certain difference between the experimental flow field conditions and the actual flow field. In addition, it's difficult to collect experimental data. Because of the limited number of sensors,

* Corresponding author: liuzhenqing@hust.edu.cn

 <http://dx.doi.org/10.28991/cej-03091125>

➤ This is an open access article under the CC-BY license (<https://creativecommons.org/licenses/by/4.0/>).

© Authors retain all copyrights.

the data can only be collected in the part of the flow field of the wind turbine, and the whole flow field information cannot be obtained. Due to the limitation of the wind tunnel laboratory site, the wind turbine wind tunnel test is based on the actual wind turbine scale model machine, so the obtained data cannot represent the actual wind field information. When scaling model wind turbine test is carried out, the similarity between the actual wind turbine and the model should be considered, the influence of the wind tunnel size on the experiment should be considered as well. Of course, the most valuable wind tunnel test should be the measurement of the full scale prototype wind turbine at all times, which requires that wind tunnel test site is large enough. At the same time, the test technology is difficult and costly. So at the moment, there is and only one full scale wind turbine test record: In 2001, the experimental research of wind turbine was carried out by the Renewable Energy Laboratory of the United States [1-2]. However, this experiment focused on the aerodynamic performance of the blade of the wind turbine, such as the pressure distribution on the blade element, and there was no experimental observation of the tail flow field of the wind turbine. In 1979, by using a hot wire anemometer to study the wind speed distribution in the wind turbine tail. Alfredsson [3], a Swedish scientist, calculated the ratio of wind turbine output, and the influence of wake on wind turbine output is revealed. Wang Yuanbo et al. [4] simulations of nine yaw and fifteen tilt control methods with the upstream turbine were carried out based on an actuator line method with Open FOAM. Around 1997, Ebert et al. [5] also used this technique to carry out a large number of wind turbine tail flow characteristics research experiments, which include tip vortex and velocity flow field. However, the experimental results show that the anemometer is unable to obtain the global instantaneous flow field information. J. Wha et al. [6] used Particle Image Velocimetry (PIV) technology to measure the wake flow of the three-blade wind turbine model in the water tank, and compared the results with the data obtained from the real wind turbine. A new method for the study of wind turbine wake was provided, but the experimental data and the actual data were quite different, and the research was mainly focused on the near wake flow field.

With the development of computer technology, computational fluid dynamics (CFD) is also widely used in numerical simulation of wind turbine wake [7-19]. Dai Dandan et al. [7] conducted numerical simulation of three-dimensional flow field on the wind impeller of single wind turbine and tandem layout of double wind turbines. Based on the RNG turbulence model, Yan Haijin [8] had carried out a simple full model numerical simulation of a single wind turbine. In his study, the results of wind velocity distribution, pressure distribution and flow separation in the whole flow field were obtained. However, the effects of blade rotation, surface and wind speed gradient on the convection field were not taken into account. And it was also difficult to divide the mesh of blade body fitting when the full model numerical simulation was carried out. Combining CFD numerical simulation method with wind turbine wake model, Li Shaohua [9] studied the wind turbine power and wake distribution of two wind turbines under the condition of seriation, juxtaposition and misalignment. He qualitatively analyzed that under the condition of serial arrangement, the wake from turbines in upwind rows can negatively impact the performance of downwind rows. However, the full model body-fitted grid was also used, the number of grids was large. Yang Rui [10] used actuating disk instead of wind wheel to carry out the numerical simulation of wind turbine tail flow. This method can simplify the mesh, and does not need to mesh the complicated fan blades. The aerodynamic drag of the wind turbines can be simulated by applying the pressure step on the actuating plate, and the power loss between the upwind direction and downwind direction wind turbine can be well simulated. However, the method only considered the axial induced force and the tangential induced force was ignored, so the information of near wake field could not be captured. Ren Huilai [11] used ADM-R to simulate the wind turbine tail flow, and qualitatively analyzed the characteristics of the wake flow field and its development process. But Ren did not compare the calculated results with the experimental data and was unable to analyze the accuracy of the method. Li Pengfei [12] used the ALM method to carry out the numerical simulation of the wind turbines wake, and analyzed the wake field information under different tip velocity ratio conditions. But the actual situation of turbulence flow was not taken into account. There were many other scholars who do similar research, such as Han Xingxing [13], Zhao Feng [14], Zhu Chong [15], Hou Yali [16], Ai Yong [17] and so on.

Although a modern wind turbine can be very large in size, e.g. >100 m in both diameter and hub height, it still operates in the lower part of the atmospheric boundary layer (ABL), where the wind is highly turbulent. In this paper, three actuating methods are developed to study wind turbine wakes. Besides, the author will analyze the flow field information under the conditions of turbulent flow, tip wind speed ratio = 5.52, 9.69, and compare the numerical simulation results with the experimental results [18] to study the respective calculation characteristics. It provides the theoretical basis for the optimal arrangement of the wind turbine.

2. Numerical Methods

Based on large eddy simulation (LES), the horizontal axis wind turbine tail flow is simulated by three kinds of actuation methods in this paper. Subgrid-scale model is adopted to simulate the effects of small-scale turbulence on large-scale turbulence. The N-S equation is averaged in a small space domain so that small-scale vortex flows are removed from the flow field and the equations satisfied by the large eddy are derived. The filtered incompressible Navier–Stokes Equations are as follows:

$$\frac{\partial \rho}{\partial t} + \frac{\partial}{\partial x_i}(\rho \bar{u}_i) = 0 \quad (1)$$

$$\frac{\partial \bar{u}_i}{\partial t} + \frac{\partial(\bar{u}_i \bar{u}_j)}{\partial x_j} = -\frac{1}{\rho} \frac{\partial \bar{p}}{\partial x_i} + \nu \frac{\partial}{\partial x_j} \left(\frac{\partial \bar{u}_i}{\partial x_j} \right) + \frac{\partial(\bar{\tau}_{ij})}{\partial x_j} + f_i \quad (2)$$

In the Upper Formula:

$$\bar{\tau}_{ij} = -\bar{u}_i' \bar{u}_j' = \bar{u}_i \bar{u}_j - \overline{u_i u_j} \quad (3)$$

The standard Smagorinsky–Lilly Model is used to calculate the Subgrid-Scale (SGS) Stresses. Based on the isotropic turbulence, it is considered that the subgrid-scale turbulence has a mixed length vortex viscosity coefficient. The specific expression is as follows :

$$\tau_{ij} - \frac{1}{3} \tau_{kk} \delta_{ij} = \mu_t \left(\frac{\partial \bar{u}_i}{\partial x_j} + \frac{\partial \bar{u}_j}{\partial x_i} \right) = 2 \mu_t \bar{S}_{ij} \quad (4)$$

Where \bar{S}_{ij} is a part of the subgrid scale isotropy, μ_t denotes the SGS turbulent viscosity force defined as follow:

$$\mu_t = C_s^2 \rho \Delta^2 \left(2 \bar{S}_{ij} \bar{S}_{ij} \right)^{\frac{1}{2}} = C_s^2 \rho \Delta^2 |\bar{S}| \quad (5)$$

Where C_s is Smagorinsky constant and chosen as 0.032 to reduce the diffusion of subgrid stress.

2.1. Actuating Disk Model (ADM)

The method only calculates the axial induced force and assumes that the axial induced force is uniformly distributed in the plane of wind wheel. According to thrust coefficient expression. Then if the thrust coefficient C_T is known, the axial induced force T can be obtained. The dynamic source term of volume force can be solved as:

$$f_x = \frac{C_T \cdot \rho U_\infty^2 A_D}{2 A_D \Delta x} = \frac{C_T \cdot \rho U_\infty^2}{2 \Delta x} \quad (6)$$

2.2. Actuator Disk Model with Rotation (ADM-R)

Based on the theory of blade element momentum (BEM), this method divides the blade into several blade elements along the radial direction, as shown in Figure 1. Then, the lift and drag on each blade element can be calculated as:

$$dL = \frac{1}{2} C_l(\alpha) \rho V_{rel}^2 c dr \quad (7)$$

$$dD = \frac{1}{2} C_d(\alpha) \rho V_{rel}^2 c dr \quad (8)$$

Where C_l and C_d are lift coefficient and drag coefficient, respectively. They can be interpolated from the local wind attack angle according to the characteristic curve of airfoil coefficient changing with the wind attack angle. The V_{rel} is the air velocity relative to the blade and can be solved by the local velocity vector triangle shown in Figure 1(b), and calculated as follows:

$$V_{rel} = \sqrt{U_\infty^2 (1-a)^2 + r^2 \Omega^2 (1+a')^2} \quad (9)$$

Where a is the axial induced factor, and a' is the tangential induction factor. Then, the thrust and moment acting on the blade element can be calculated as:

$$dT = dL \cos \varphi + dD \sin \varphi = \frac{1}{2} \rho V^2 B c (C_L \cos \varphi + C_D \sin \varphi) dr \quad (10)$$

$$dQ = (dL \sin \varphi - dD \cos \varphi) r = \frac{1}{2} \rho V^2 B c (C_L \sin \varphi - C_D \cos \varphi) r dr \quad (11)$$

According to the momentum theorem and angular momentum theorem, the reaction force and moment of the airflow acting on the blade element can be obtained as follows:

$$dT = 2\pi r dr \cdot \rho U_\infty (1-a) 2a U_\infty \quad (12)$$

$$dQ = 2\pi r dr \cdot \rho U_\infty (1-a) 2a' r^2 \Omega \quad (13)$$

After simultaneous solving of Formula (10), (11), (12), (13), the a and a' can be obtained iteratively. Since the BEM theory assumes that the wingspan direction is infinitely large and the momentum theory is only applicable to the case where the axial induction factor is relatively small, the Prandtl loss factor and the Grawert loss factor [16] are introduced to modify the induction factor in this paper.

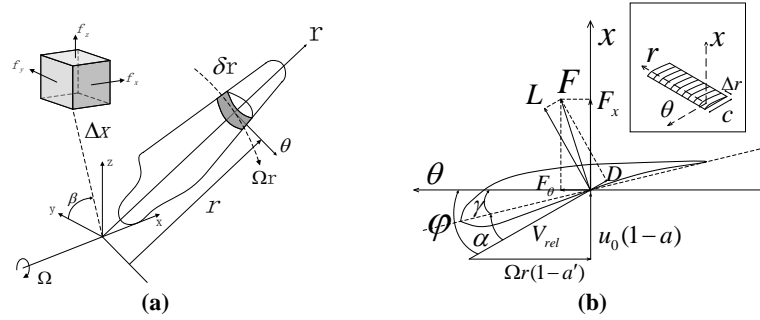


Figure 1. BEM theoretical analysis diagram: (a) Blade appearance; (b) Blade element force diagram

Decomposing lift and drag into axial forces dF_x and tangential forces dF_θ , as shown in Figure 1. Then the axial and tangential inductive forces on the three blades are averaged along the radial micro ring, and the dynamic source term of the volume force is calculated as:

$$f_x = -\frac{B}{2\pi r} \frac{dF_x}{\Delta x \delta r} \quad (14)$$

$$f_\theta = -\frac{B}{2\pi r} \frac{dF_\theta}{\Delta x \delta r} \quad (15)$$

2.3. Actuator Line Model (ALM)

The ADM-R method assumes that induced force is uniformly distributed in the radial micro ring of the wind turbine. ALM method gives up such assumption. For a given tip velocity ratio, ALM method can be used to calculate the rotating angular velocity of the wind wheel. Thus, ALM method can determine the grid swept by each blade at any time, and then the volume force term is applied to the corresponding grid. The solution of induced force is the same as ADM-R method, which is based on BEM theory. Dynamic source term of the volume force is calculated as:

$$f_x = dF_x / V, \quad f_\theta = dF_\theta / V \quad (16)$$

Where V represents the volume of the blade sweeping through the grid.

3. Numerical Model

3.1. Object of Study and Boundary Conditions

The 1/100 scaled model wind turbine of MWt-1000 [10] is used in this study. The radius of the model is 0.285 m and the hub height is 0.7 m. The size of model is shown in Figure 2(a). The longitudinal length of the computational domain is 13.5 m, the height is 1.8 m and the transverse length is 1.5 m. The wind turbine is located 8.5 m downstream from the inlet. The downstream area of the wind turbine extends to 5 m in the longitudinal direction. At a distance of 6 m away from the wind turbine, three wedges are arranged to simulate the atmospheric boundary layer conditions with turbulence, as shown in Figure 2(b). At the inlet, a uniform wind speed, 10 m/s, is provided, i.e. $u=10$ m/s, $\partial p / \partial n=0$. The pressure-outlet condition is specified at the outlet, i.e. $p=0$, $\partial u / \partial n=\partial v / \partial n=\partial w / \partial n=0$. The symmetry conditions are used at the top and side of the computational domain, i.e. $\partial u / \partial n=\partial v / \partial n=\partial w / \partial n=\partial p / \partial n=0$. And at other boundaries, the wall boundary conditions are used, i.e. $u=v=w=0$, $\partial p / \partial n=0$.

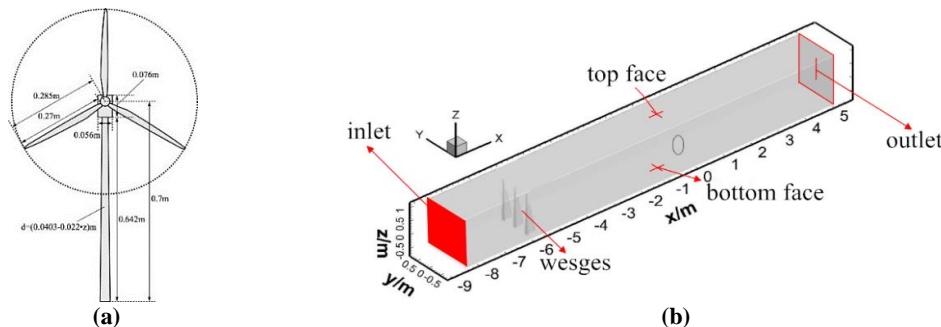


Figure 2. Numerical model: (a) The wind turbine model (b) Schematic of the computational domain

3.2. Grid System and Conditions

In this study, total mesh number of the global calculation domain is 2.5×10^6 , the minimum grid size is 3 mm and the maximum grid size is 25 mm, the grid system is shown as Figure 3. Considering the large change gradient of velocity, smaller mesh is needed near the bottom of the calculation domain, the wind turbine and the wedges, in order to capture the characteristics of the flow field, so local refinement is done. The vertical size of grids in the bottom of the calculation domain is 5 mm, and the vertical grid growing ratio is 1.2. In longitudinal direction, the size of the grids near the wind turbine is 5 mm, and the grid growing ratio is 1.1. On the wedges surface, the minimum grid size is 3 mm and the maximum grid size is 15 mm.

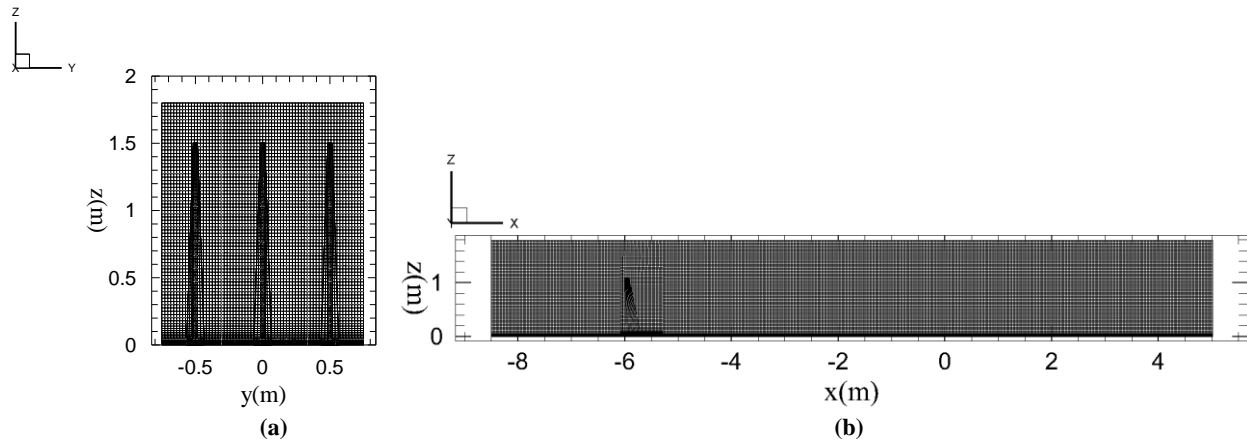


Figure 3. Mesh of the numerical model: (a) Lateral view (b) Elevation view

In this study, two conditions are carried out. The first one is that the blade tip velocity ratio λ is valued 5.52 when the wind turbines work with rated power, and the other is $\lambda=9.69$ when the maximum generating efficiency of the wind turbine is reached. The wind velocity of inlet is 10 m/s, as shown in Table 1.

Table 1. Calculation cases

Case name	λ	wind velocity (m/s)
Case1	5.52	10
Case2	9.69	10

4. Numerical Results

4.1. Accuracy Verification of Grid System

To ensure that the turbulent wind farm was in accordance with the experimental conditions, numerical simulation was firstly done with the absence of the wind turbine to verify the accuracy of the grid system. The distribution of velocity simulated by LES was used to show the characteristics of the flow field. The computation time step was set to 0.0001 s, the maximum number of iterations was 20 times in each time step, and the statistical time was about 7 s. At the center of the wind turbine, the mean velocity of numerical result was 10.55 m/s, which matches well with it (10.58 m/s) in the experiment. The axial mean velocity and fluctuating velocity were extracted from the section of $y=0$, and dimensionless processing was done by dividing the mean velocity at center of the wind turbine. The mean velocity contour and the non-dimensional mean velocity profile as well as the fluctuating velocity contour and the non-dimensional fluctuating velocity profile are shown in the Figure 4. The location of mean velocity profile and the fluctuating velocity profile are $x = 0, 2D, 4D, 6D$.

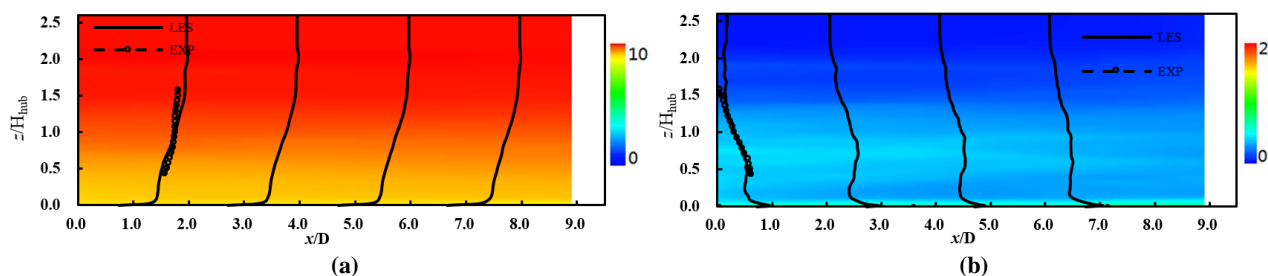


Figure 4. The wind field distribution: (a) Axial mean velocity contour (b) Fluctuating velocity contour

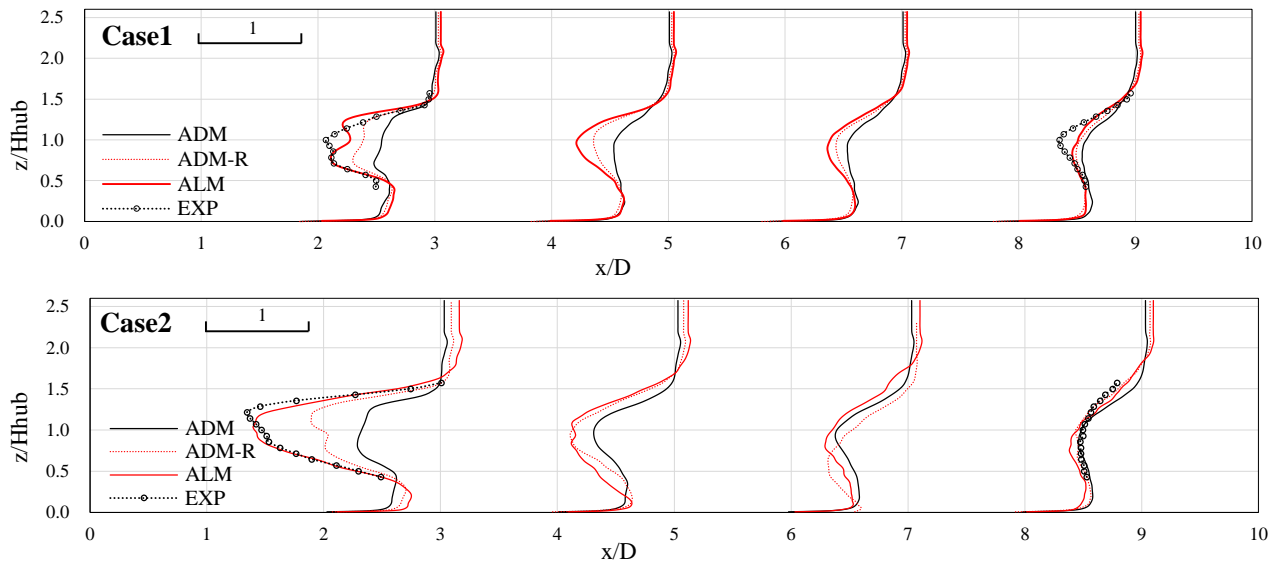


Figure 5. The axial wind profile

4.2. Flow Field Analysis of Three Actuation Methods

The results of three actuation methods are compared in this part. The axial mean wind velocity and fluctuating wind velocity are extracted at profile ($y=0$). The non-dimensional mean wind velocity profile is shown in Figure 5, and the non-dimensional fluctuating velocity is in Figure 6. The sections of profile are at $x=2D$, $4D$, $6D$, $8D$, respectively. According to Figure 5, the wind speed decreases rapidly after the wind passes through the plane of the wind turbine. And the farther away from the wind turbine, the weaker the disturbance effect of the wind turbine to the wind field will be. At the center of the wind turbine, the wind speed is the smallest and gradually increases upward and downward, which is consistent with the experimental trend. The closer to the wind turbine, the greater difference between calculations results of three actuation methods are. The results of the three actuation methods at $x=6D$ are basically consistent. At the same time, it is found that the greater the blade tip velocity ratio, the greater the obstruction of the wind turbine and the smaller the wind speed at the same location. The numerical result of ADM and experimental values vary greatly in near wake area. In the meanwhile, ADM-R results match better with experimental data than ADM, and ALM matches best. In the far wake region, the results of three methods are similar and are in good agreement with the experimental data. That is because that ADM assumes uniform distribution of axial induced force on wind turbine plane and ignore tangential induction force, which means the rotation effect is neglected. Therefore, the near wake flow field error is large, and it cannot capture near wake flow information. Although tangential induction is considered in ADM-R method, it assumes that induction force is uniformly distributed in the radial micro ring of the wind turbine, which is not consistent with the actual situation. So the results of ADM-R have large error near the wake. Different from the former two assumptions, ALM method directly exerts axial and tangential inductive forces on the grid swept by the blade of the wind turbine, so the calculated results are closer to the experimental values. And it can be found that when the blade tip velocity ratio is larger, the calculated results of the ALM method are more consistent with the experimental results. However, in the far wake flow field, the calculation results of the three methods are similar and are basically consistent with the experimental values. At the center of the wind wheel, the calculation results deviated from the experimental values because the obstruction effect of the wind turbines was not considered in this study.

In Figure 6, it shows that after the wind passed through the plane of the wind turbine, the fluctuating velocity increases. At the place farther away from the fan, the disturbance effect of fans on wind field is weakened and the fluctuating velocity decreases. The maximum of the fluctuating velocity occurs at blade tip, and the fluctuating velocity gradually decreases upward and downward, which shows good agreement with experiment. The larger the blade tip velocity ratio is, the more obvious the disturbance effect of wind turbine on flow field can be, and the higher fluctuating velocity will be. The three actuating methods calculation results of the fluctuating velocity are quite different between near wake flow field and the far wake flow field. Comparing the three kinds of actuating models, it can be seen that ADM method has the biggest error compared with experiment however and the error of ADM-R method is between the other two methods, ALM shows the best agreement with experiment. According to the comprehensive performance of the mean wind field and the fluctuating wind field predicted by the three kinds of actuating models, the ALM method results are the most reliable. Therefore, the wake wind field obtained by the ALM method is used for further momentum balance analysis.

Under the two conditions, the axial mean velocity contours calculated by three method in several sections ($x=D$, $2D$, $4D$, $6D$) are plotted in Figure 7. As shown in Figure 7, the influence region of the wind turbine in the original flow field is similar to the cylindrical flow tube with the same diameter as the wind turbine. After flow passing through the wind

turbine, the velocity of the airflow decreases rapidly and then recovers gradually. The wind speed is basically stable at $x = 6D$. Because of the different assumptions of the three methods, the axial mean velocity calculated by ADM method shows circular uniform distribution, which is in sake of that ADM does not take the effect of the wind wheel rotation into account. Unlike the results of ADM, the axial velocity obtained by ADM-R and ALM is basically circular distribution. Due to the influence of wind shear, the axial velocity is not completely symmetrical distribution. The axial velocity calculated by ADM is smallest among the three methods. And it has great difference with that of the other two methods. However, the calculated values of the three methods show little difference in the region of the far wake (about $x \geq 6D$).

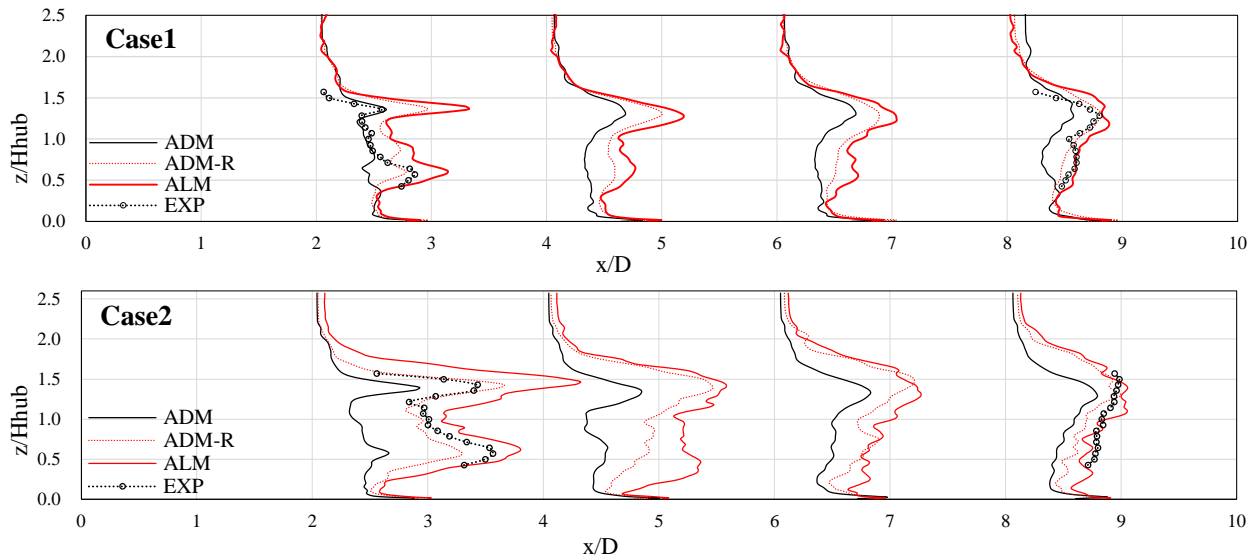


Figure 6. The fluctuating velocity profile

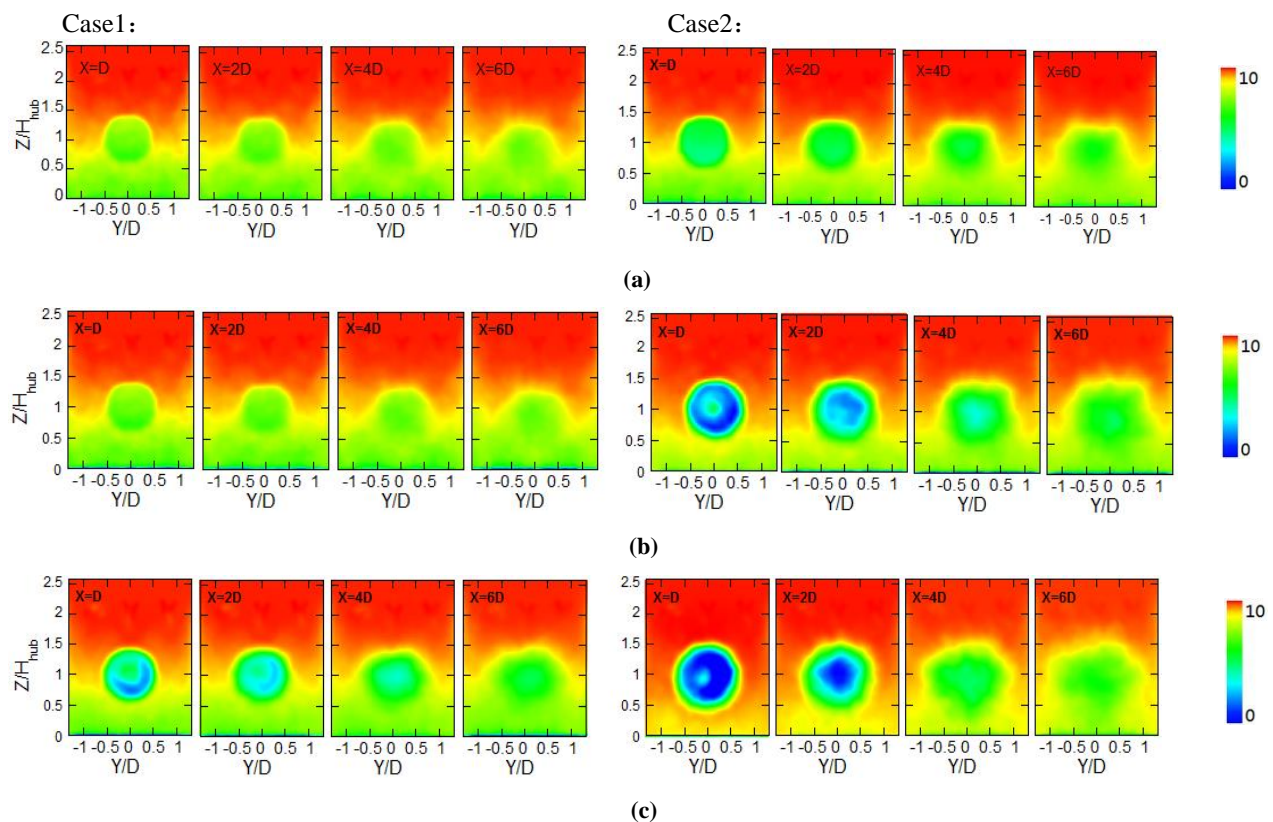


Figure 7. The contour of mean velocity in several sections: (a) ADM (b) ADM-R (c) ALM

4.3. N-S Equation Equilibrium Analysis of ALM

By time averaged data process of N-S equation, the time-averaged momentum equation in the downwind direction is shown in Formula (17):

$$\bar{u}_i \frac{\partial \bar{u}}{\partial x_i} = -\frac{1}{\rho} \frac{\partial \bar{p}}{\partial x} - \frac{\partial u'u'_i}{\partial x_i} + D_u \quad (17)$$

Where $\bar{u}_i \frac{\partial \bar{u}}{\partial x_i} = \bar{u} \frac{\partial \bar{u}}{\partial x} + \bar{v} \frac{\partial \bar{u}}{\partial y} + \bar{w} \frac{\partial \bar{u}}{\partial z}$ is the convection term, $\frac{\partial u'u'_i}{\partial x_i} = \frac{\partial u'u'}{\partial x} + \frac{\partial u'v'}{\partial y} + \frac{\partial u'w'}{\partial z}$ is the turbulent stress term, D_u is the diffusion term.

At the center of wind turbine, the distribution along the downwind direction of each terms of N-S Equation are plotted in Figure 8 and the distribution curves of each sub item are shown in Figure 9. According to the curves in Figure 8, the turbulent stress term, pressure gradient term and convection term mainly contribute to the equation equilibrium at near wake, and the diffusion term is very small. As the distance away from the wind turbine increases, the pressure gradient term decreases gradually, and the pressure become stable at about 3D. In the far wake region, the convection term is in equilibrium with the turbulent stress term. It shows that the larger the wind speed ratio of blade tip is, the larger each item of turbulence stress is in the region of near wake flow field ($x < 6D$). But the values of each term are almost identical in the far wake region. In Figure 10, the main action of the convection term is in the x direction, and the other two are basically zero. And in the convection terms, regardless of the blade tip velocity ratio, the x convection term always dominates, and the contribution of the remaining sub-terms can be ignored. In the range of $x < 2D$ for turbulent stress term, the turbulence stress in all three directions is relatively large, and the turbulent stress in the x direction is basically zero in the range of $x > 2D$.

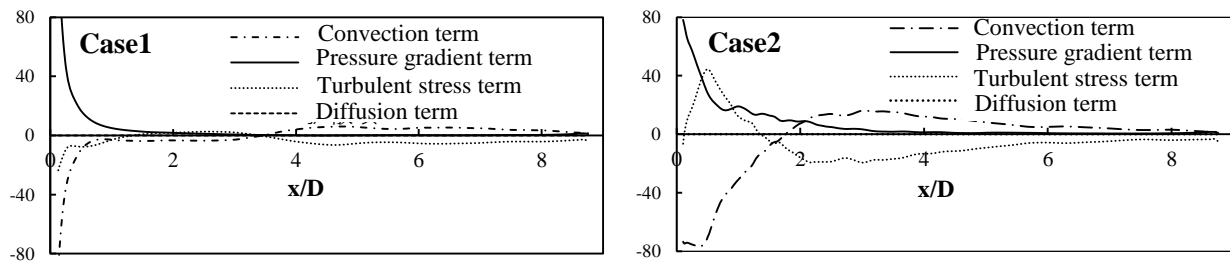


Figure 8. N-S equation equilibrium curves

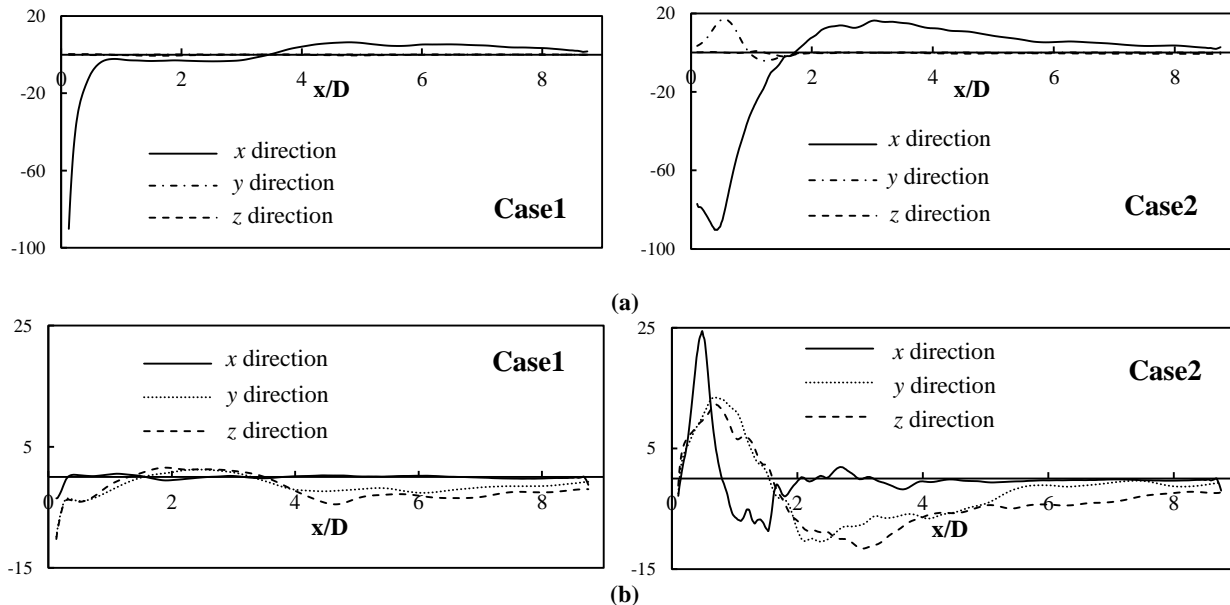


Figure 9. Distribution curves of each term: (a) Distribution curve of convection terms; (b) Turbulence curve of convection terms

In profile of $z = 0$, N-S equation equilibrium relation in several sections are plotted in Figure 11, i.e. $x=2D, 4D, 6D, 8D$. In Figure 10(a), with the wind turbine not placed, in the area $x>0$, the pressure gradient term is basically zero, the convection term and the turbulent stress term remain basically unchanged, and both are very small. The convection term and the turbulent stress term mainly contribute to the equation equilibrium. However, when the wind turbine is placed, the values of the three terms increase sharply. At low blade tip velocity ratio ($\lambda=5.52$), the pressure gradient term is very

small, and the equilibrium is mainly provided by the turbulent stress term and convection term. For the high blade tip velocity ratio ($\lambda=9.69$), the pressure gradient only works in the near wake, and is very small in the far wake. With the blade tip wind speed ratio increases, the value of three terms increase in the near wake region ($x < 4D$), but in the region of the far wake, i.e. $x > 4D$, the difference of each terms is not significant.

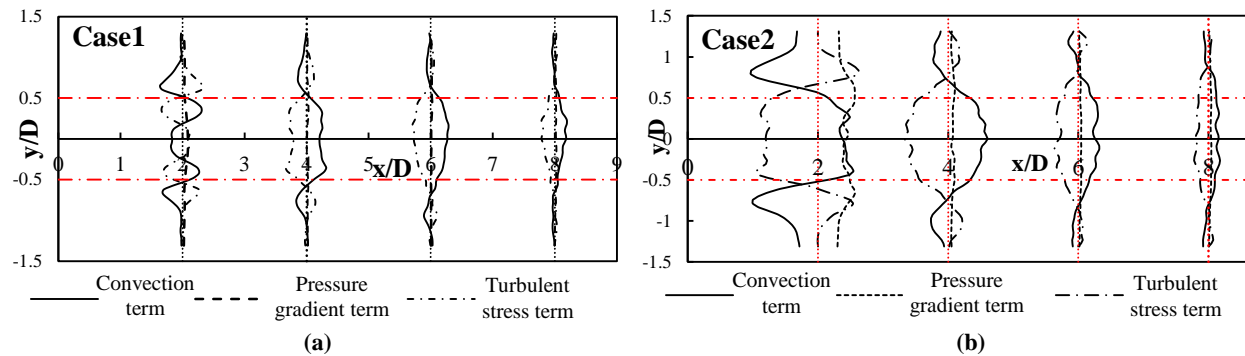


Figure 10. Equilibrium curves of N-S equation in several sections: (a) Low blade tip velocity ratio; (b) High blade tip velocity ratio

4.4. Computing Resources

The large eddy simulation (LES) takes a lot of computing resources. It will take about 120 hours to accomplish the numerical simulation of entire flow field without effects of wind turbine under the parallel computing condition of 16-core I7-5960X CPU. The computing time will increase when considering the effects of wind turbine on flow field. Table 2 lists the computing time of iterating 100 time steps with the same grid system and same computer configuration, in which the time step is set to 0.0001s. It is obvious that ADM method takes the shortest time, which is 3.86% higher than that without the wind turbine, ADM-R method is the second, increasing by 10.45%, and ALM method takes the longest time, increasing by 25.70%. ADM method assumes that the axial inductive force is uniformly distributed, and ADM-R method assumes that inductive force is uniformly distributed in a micro radial ring. In the process of computation, dynamic source term of volumetric force applied by these two methods remains constant. But volume force applied by ALM method varies with time, and the obtained fluctuating velocity is larger, the flow field is more disordered, so the calculation speed is slower.

Table 2. Computing conditions

Case name	Without wind turbine	ADM	ADM-R	ALM
Time-consuming	1934	2018	2146	2431
Increasing ratio		4.34%	10.96%	25.7%

5. Conclusion

In this paper, three actuator methods combined with LES model are used to simulate the wind turbine wake flow fields. The results of numerical simulation and experiment are compared. The characteristics of these actuator methods are examined and the momentum balance of the wake flow is studied. The following conclusions were reached:

- Sharp wedges are placed in front of a wind turbine to simulate inflow turbulence conditions. The results of numerical simulation is in good agreement with the experimental results, which verifies the accuracy of the numerical model adopted in this study.
- After the flow encounters the wind turbine, the mean wind velocity decreases rapidly while the fluctuating wind velocity increases. With the increase of the distance away from wind turbine, the initial state are restored, the mean wind speed increases and the fluctuating wind speed decreases. Besides, the wind speed is basically stable at about $x=6D$. It is found that the larger the blade tip wind speed ratio is, the stronger the disturbance of the wind turbine to the original flow field will be.
- The simulation accuracy of three actuator methods under different blade tip wind speed ratios is examined. In the region of near wake flow field, both ADM-R and ADM methods have great error with the experimental data, and cannot capture the information of near wake flow field. ALM method is in good agreement with the experimental data for both the mean and the fluctuating flow fields.

- Contribution from each term in N-S equation of the wind turbine wake are revealed. The turbulent stress term, pressure gradient term and convection term play the major role at near wake region. In the far wake region, the convection term balances with the turbulent stress term.

6. Funding

The authors thank the supports from the Guangdong Power Grid Company Limited R&D project (No.GDKJQQ20161150).

7. References

- [1] Hand, M. M., Simms, D. A., Fingersh, L. J., Jager, D. W., Cotrell, J. R., Schreck, S., and Larwood, S. M.. "Unsteady Aerodynamics Experiment Phase VI: Wind Tunnel Test Configurations and Available Data Campaigns." United States (December 2001). doi:10.2172/15000240.
- [2] Schreck S. "The Nrel Full-Scale Wind Tunnel Experiment Introduction To The Special Issue." Wind Energy 5 (July 2002): 77-84. doi:10.1002/we.72.
- [3] Alfredsson, P.H. and J.A. Dahlberg. "A Preliminary Wind Tunnel Study of Windmill Wake Dispersion in Various Flow Conditions." Part 7 (1979).
- [4] Wang Yuanbo, Li Chun, Yan Weirun, et al. "Research on Wind Turbine Control Strategy Based on Power Output of Whole Wind Field." Proceeding of the CSEE 37 (August 2017): 4437-4445. doi:10.13334/j.0258-8013.pcsee.161233.
- [5] Ebert, P.R. and D.H. Wood. "The Near Wake of A Model Horizontal-Axis Wind Turbine—II. General Features of The Three-Dimensional Flow Field." Renewable Energy 8 (December 1999): 513-534. doi:10.1016/S0960-1481(98)00797-6.
- [6] Dave Simms, Maureen Hand, Dave Jager, Jason Cotrell, Mike Robinson, Scott Schreck, Scott Larwood, and Lee Fingersh. "Wind Tunnel Testing of NREL's Unsteady Aerodynamics Experiment." 20th 2001 Asme Wind Eergy Symposium. doi:10.2514/6.2001-35.
- [7] Dai Dandan, Ma Bo, He Yan. "Research on Wind Turbine Trail Characteristics Based on Fluent." Mechanical Engineering & Automation 4 (August 2017):10-12.
- [8] Yan Haijin, Hu Danmei, Li Jia. "Numerical Simulation of Flow Field in Impeller of Horizontal Axis Wind Turbine." Journal of Shanghai University of Electric Power 2 (April 2010): 123-126. doi:10.3969/j.issn.1006-4729.2010.02.006.
- [9] Li Shaohua, Yue Weipeng, Kuang Qingfeng, Wu Dianwen, Wang Chengyin. "Numerical Simulation of Double Turbine Wake Interaction and Array." Proceedings of the CSEE 5 (February 2011): 101-107. doi: 10.13334/j.0258-8013.pcsee.2011.05.019.
- [10] Yang Rui, Xia Wei, Wang Tingting, Li Jinlong. "Application of Actuating Disk Model in Wind Farm." Journal of Lanzhou University of Technology 1 (May 2016): 66-69. doi:10.3969/j.issn.1673-5196.2016.01.014.
- [11] Ren Huilai, Zhang Xiaodong, Kang Shun. "Simulation Analysis of Wind Turbine Tail Flow Based on Non-uniform Actuation Disk." Hydroelectric Energy Science 35 (February 2017): 193-195.
- [12] Li Pengfei, Liu Jiancheng. "Numerical Simulation of Wake Field of Wind Turbine Based on Actuation Line Model." Chinese Journal of Hydrodynamics 31 (March 2016):127-134. doi:10.16076/j.cnki.cjhd.2016.02.001.
- [13] Han Xingxing, Xu Chang, Liu Deyou. "Actuator Disk Model of Wind Farms Based on the Rotor Average Wind S peed." Journal of Engineering Thermophysics 37 (March 2016): 501-506.
- [14] Zhao Feng, Duan Wei. "Loading Analysis and Strength Cacluation of Wind Turbine Blade Based on Blade Element Momentum Theory and Finite Element Method." Machinery Design & Manufacture 8 (August 2010): 42-44. doi:10.19356/j.cnki.1001-3997.2010.08.019.
- [15] Zhu Chong. "Numerical Simulation of Wake Flow Field of Wind Turbine." Nanjing University of Aeronautics and Astronautics (2012).
- [16] Hou Yali, Wang Jianwen, Wang Qiang, Wang Xinting. "Effect of Wind Shear on the Wake Turbulence Characteristics of the Wind Turbine." Journal of Mechanical Engineering 16 (August 2016): 149-155. doi:10.3901/JME.2016.16.149.
- [17] Ai Yong, Cheng Ping, Wan Decheng. "Numerical simulation of the wake field of staggered two fans based on actuating line model." Ocean Engineering 36 (January 2018):27-36.doi:10.16483 /j.issn.1005-9865.2018.01.004.
- [18] Ishihara Meng, Qian Qiwei. "Numerical Prediction of Wind Turbine Wake and Proposal of Analytical Model." Symposium on Wind Engineering Symposium Proceedings of 24th Wind Engineering Symposium the Japan Wind Cooperation Association (2016): 151-156.
- [19] Martin O L H.. "Aerodynamics of Wind Turbines." Xiao Jinsong, translated. Beijing: China Electric Power Press (2009).